Cardiovascular Research (2011) **90**, 105–112
doi:10.1093/cvr/cvq379

T-type Ca^{2+} signalling regulates aldosterone-induced CREB activation and cell death through PP2A activation in neonatal cardiomyocytes

Laurent Ferron[1†], Yann Ruchon[1,2], Jean-François Renaud[1,2], and Véronique Capuano[1,2*]

[1]Département de Recherche Médicale, Remodelage tissulaire et fonctionnel: signalisation et physiopathologie CNRS-UMR8162, Le Plessis Robinson, France; and [2]INSERM-U999, Université Paris-Sud XI, Hôpital Marie Lannelongue, 133 ave de la Résistance, 9230 Le Plessis Robinson, France

Received 12 May 2010; revised 8 November 2010; accepted 25 November 2010; online publish-ahead-of-print 30 November 2010

Time for primary review: 31 days

Aims We have investigated Ca^{2+} signalling generated by aldosterone-induced T-type current (I_{CaT}), the effects of I_{CaT} in neonatal cardiomyocytes, and a putative role for I_{CaT} in cardiomyocytes during cardiac pathology induced by stenosis in an adult rat.

Methods and results Neonatal rat cardiomyocytes treated with aldosterone showed an increase in I_{CaT} density, principally due to the upregulation of the T-type channel $Ca_v3.1$ (by 80%). Aldosterone activated cAMP-response element-binding protein (CREB), and this activation was enhanced by blocking I_{CaT} or by inhibiting protein phosphatase 2A (PP2A) activity. Aldosterone induced PP2A activity, an induction that was prevented upon I_{CaT} blockade. I_{CaT} exerted a negative feedback regulation on the transcription of the $Ca_v3.1$ gene, and the activation of PP2A by I_{CaT} led to increased levels of the pro-apoptotic markers caspase 9 and Bcl-x_S and decreased levels of the anti-apoptotic marker Bcl-2. These findings were corroborated by flow cytometry analysis for apoptosis and necrosis. Similarly, in a rat model of cardiac disease, I_{CaT} re-emergence was associated with a decrease in CREB activation and was correlated with increases in caspase 9 and Bcl-x_S and a decrease in Bcl-2 levels.

Conclusion Our findings establish PP2A/CREB as targets of I_{CaT}-generated Ca^{2+} signalling and identify an important role for I_{CaT} in cardiomyocyte cell death.

Keywords Apoptosis • Cav3.1 channel • Gene expression • Glucocorticoid receptor • Protein phosphatase

1. Introduction

Ca^{2+} entry through T-type channels was reported to have two main roles, one related to cell excitability and the other to the stimulation of a range of Ca^{2+}-dependent biological events.[1–3] In ventricular cardiomyocytes, both $Ca_v3.1$ and $Ca_v3.2$ channel subunits are responsible for I_{CaT}, and the pattern of expression of these channels varies with the stage of heart development.[4–6] The reappearance of I_{CaT} in adult cardiomyocytes was reported, in association with several aetiologies of ventricular hypertrophy.[3] However, little is known about the mechanism involved in the regulation of T-type channel expression, and the I_{CaT}-dependent Ca^{2+} signalling pathway remains to be explored.

It has repeatedly been demonstrated that $Ca_v3.1$ and $Ca_v3.2$ are regulated differently and have different cellular functions. Consistent with this observation, mice lacking $Ca_v3.1$ have a cardiac phenotype different from that of mice lacking $Ca_v3.2$ and, similarly, mice overexpressing the $Ca_v3.1$ gene have a response to hypertrophic stimuli very different from that of mice overexpressing the $Ca_v3.2$ gene.[7,8] However, the role of I_{CaT} in the development of cardiac hypertrophy remains a matter of debate, as does the identity of the channel subunit involved. Indeed, Chiang *et al.*[7] reported that cardiac hypertrophy was

† Present address: Laboratory of Cellular and Molecular Neuroscience, Department of Neuroscience, Physiology and Pharmacology, University College London, London, UK.

* Corresponding author. Tel: +33 1 40 94 25 23; fax: +33 1 40 94 25 22, Email: veronique.capuano@ccml.u-psud.fr

associated with $Ca_v3.2$ expression (but not with $Ca_v3.1$ expression), whereas Nakayama *et al.*[8] described an anti-hypertrophic role for $Ca_v3.1$. Our previous work with an *in vivo* model provided evidence that the pathological re-expression of $Ca_v3.1$ and, to a lesser extent, $Ca_v3.2$ channels was independent of cardiac hypertrophy *per se*, and we suggested that I_{CaT} might be associated with end-stage organ damage during cardiac disease.[9] Consistent with this hypothesis, the use of mibefradil, an I_{CaT} antagonist, was shown to improve survival in a rat model of chronic heart failure such as sudden death and fibrillation, suggesting that I_{CaT} blockade might have a beneficial impact on cardiac diseases.[10,11]

Aldosterone is known to be involved in the development of cardiac hypertrophy and failure, and was described as participating in electrophysiological remodelling in ventricular myocytes, increasing both L-type Ca^{2+} current (I_{CaL}) and I_{CaT}.[12,13] In this study, we used aldosterone to investigate the mechanisms involved in channel gene expression, to identify the signalling pathways triggered by I_{CaT}-generated Ca^{2+} influx, and to determine the cellular impact of I_{CaT}-generated Ca^{2+} signalling in cardiomyocytes. We found that aldosterone-dependent I_{CaT}-generated Ca^{2+} signalling induced negative feedback on cAMP-response element-binding protein (CREB) via protein phosphatase 2A (PP2A). Through its targeting of PP2A, I_{CaT} increased pro-apoptotic markers and cell death. These findings implicate I_{CaT} in the regulation of CREB-dependent gene expression and I_{CaT}/PP2A/CREB signalling in promoting apoptosis.

2. Methods

2.1 Animals and culture conditions

Animals were cared for and used in accordance with the European convention for the protection of vertebrates used for experimental purposes, and institutional guidelines no. 86/609/CEE 24 November 1986 and conforms to the Guide for the Care and Use of Laboratory Animals published by the US National Institutes of Health (NIH Publication no. 85-23, revised 1996). Primary cultures of ventricular myocytes were each prepared from hearts of 10 1-day-old male Wistar rats (Charles Rivers, France) as described previously.[9] Following tissue digestion, cells were plated (low density, 1 h at 37°C) in normal growth medium to isolate cardiomyocytes from adherent cells. Non-adherent cells were collected, plated on new dishes, and maintained in serum-free DMEM supplemented with medium 199 (4:1) and 1 μM cytosine β-D-arabinofuranoside (Sigma), to prevent proliferation of residual non-myocytes. Cells were exposed to aldosterone or pre-treated with antagonists or inhibitors prior to addition of aldosterone. The antagonists or inhibitors used were RU 38486 spironolactone, mibefradil, flunarizine, fluoxetine, or nifedipine all from Sigma, FK506, or okadaic acid (OA) from Alexis Biochemicals (San Diego, CA, USA) and dexamethasone from Sigma.

The hypertrophic model was described elsewhere.[9] Briefly, adult male Wistar rats were subjected to abdominal aortic stenosis for 6 (AS6) or 12 weeks (AS12) and controls were age-matched sham-operated rats (Ctl6 and Ctl12). The left ventricles were isolated, rapidly frozen, and stored at −80°C.

2.2 Electrophysiological recordings

Ca^{2+} currents were recorded by whole-cell patch-clamp technique, at room temperature (22–24°C). The fire-polished pipettes used had a resistance of 1–3 MΩ when filled with pipette solution: 10 mM CsCl, 120 mM Cs-aspartate, 3 mM $MgCl_2$, 10 mM HEPES, 15 mM EGTA, 1.8 mM $CaCl_2$, 10 mM glucose, 3.6 mM creatine phosphate, 5 mM MgATP, 0.2 mM Tris-GTP, pH 7.2, adjusted with CsOH. Ca^{2+} currents were recorded in an external solution containing: 135 mM TEA-Cl, 1 mM $MgCl_2$, 10 mM $CaCl_2$, 10 mM HEPES, 10 mM glucose, 3 mM 4–aminopyridine, 20 mM CsCl, 0.03 mM tetrodotoxin, pH 7.4, adjusted with CsOH. Additional details of data recording were reported elsewhere.[5]

2.3 Transfection and luciferase assay

The 3 kb region upstream from *cacna1g* was isolated from Wistar rat genomic library (λ DASH II, Stratagene) and inserted into the luciferase reporter pGL3-basic vector (Promega, Madison, WI, USA) as described previously.[14] The resulting plasmid was used to generate chimeric pGL promoter/luciferase constructs (pGL4100–pGL4600). The GRE1 mutant (853 bp upstream from the translation start site) resulted from a point mutation generated in pGL4400 by PCR with 5′TGGAAGG GCGTCC(T)A(C)TGGA3′ used as the primer. Neonatal myocytes were cotransfected using luciferase construct and pSVβgal (Promega) with FuGENE 6 (Roche, Indianapolis, NI, USA). Luciferase and β-galactosidase activities were determined in a related reporter assay system (Promega). All experiments were performed on at least three cultures set up in triplicate.

2.4 RNA isolation and mRNA quantification

Total RNA samples were prepared from ventricular tissues using Trizol (Invitrogen). The $Ca_v3.1$, $Ca_v3.2$, cyclophylin primers, and quantitative RT–PCR procedures have been described elsewhere.[5,15] Briefly, quantitative RT–PCR was performed with a normalized RNA aliquot (1 μg) and a known amount of cRNA internal control (2.5×10^6 molecules). The internal control differed from the target counterpart by only one restriction site. PCR was performed with a trace amount of ^{32}P-labelled 5′ primer. The number of copies per micrograms of total RNA was calculated using the following equation: [Internal control weight/(size in nucleotides × 330)] × 6.02×10^{23}, and from the relationship [molecules cRNA control/cpm cRNA control] × cpm target = target molecules per normalized RNA aliquot.

2.5 Protein extraction and western blot analysis and phosphatase activity assay

The preparation of cytosolic, nuclear, and total extracts were described elsewhere.[14] Antibodies were glucocorticoid receptor (GR), Bcl-x_L Bcl-x_S, Bcl-2 (Santa Cruz Biotechnology, CA, USA), total CREB, Ser-133-phosphorylated CREB (pCREB), caspase 9 (Cell Signaling Technology, MA, USA), which detects the pro-caspase 9 as well as the cleaved fragment of caspase 9, catalytic subunit of PP1 (Santa Cruz Biotechnology), PP2AC, and PP2B (Cell Signaling Technology). Actin (Santa Cruz) was used for normalization. Protein bands were visualized with the Lumi-light^{Plus} blotting Kit (Roche) and analysed with Gene Tools from Syngen (Cambridge, UK). The activity of PP2A was measured with the Ser/Thr phosphatase assay system (Promega). Phosphatase activity was calculated as the rate of Pi release from pre-phosphorylated peptide and normalized with respect to basal levels (sample without phosphopeptide).

2.6 Flow cytometry

For each treatment, cells were collected after digestion with trypsin. Samples from each cell suspension were stained with fluorescein isothiocyanate (FITC)-conjugated annexin V; propidium iodide (PI) exclusion assay (PI-Pharmingen) was carried out according to the manufacturer's protocol. For each sample, 30 000 cells were analysed on an FACSCalibur machine, with CELLQuest software (Becton Dickinson, Franklin Lakes, NJ, USA). Counts are expressed as a percentage of the total number of cells counted.

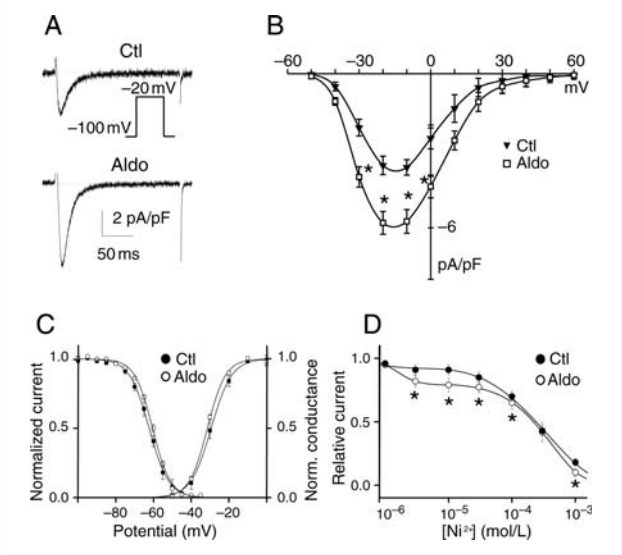

Figure 1 Aldosterone increases principally $Ca_v3.1$-generated T-type calcium current. (*A*) Typical recordings are shown for control (Ctl) and aldosterone treatment (Aldo, 1 μM). (*B*) I_{CaT} density–voltage relationships in Ctl ($n = 8$) and Aldo ($n = 15$). (*C*) Voltage-dependent activation (squares) and steady-state inactivation (circles) curves. Activation: $V_{0.5} = -27.0 \pm 2.6$ mV, $k = 5.8 \pm 0.5$ mV for Ctl ($n = 6$); $V_{0.5} = -31.4 \pm 0.4$ mV, $k = 4.8 \pm 0.1$ mV for Aldo ($n = 11$). Inactivation $V_{0.5} = -63.7 \pm 1.5$ mV, $k = -4.3 \pm 0.2$ mV for Ctl ($n = 6$); $V_{0.5} = -60.4 \pm 0.5$ mV, $k = -4.7 \pm 0.1$ mV for Aldo ($n = 8$). (*D*) Dose–response curves for Ni^{2+} on I_{CaT} recorded from a holding potential of −100 mV to a test pulse of −20 mV. $n = 5$–10 cells for each Ni^{2+} concentration. For Ctl, the IC_{50} is 300 μM. For aldosterone, two IC_{50} values were determined: 1.5 and 300 μM. $^*P < 0.05$ vs. Ctl.

2.7 Statistical analysis

Data are expressed as means ± SEM ($n \geq 3$). The statistical significance of differences between groups was estimated by one-way ANOVA, followed by Dunnett's test or two-way ANOVA, followed by Bonferroni's test. Differences were considered significant if $P < 0.05$.

3. Results

3.1 Aldosterone increases $Ca_v3.1$-related current

Cultures of ventricular myocytes treated with aldosterone for 48 h displayed an increase in I_{CaT} current density (5.7 ± 0.5 pA/pF $n = 15$ vs. 3.6 ± 0.3 pA/pF $n = 8$ in the control, $P < 0.01$; *Figure 1A* and *B*) that was not associated with changes in activation or in steady-state inactivation parameters (*Figure 1C*). The nature of the $Ca_v3.X$-related current induced by aldosterone was determined on the basis of the Ni^{2+} sensitivity of I_{CaT} (*Figure 1D*). The Ni^{2+} dose–response in control conditions indicated that I_{CaT} was blocked in the monophasic mode, with an IC_{50} of 300 μM, whereas, in aldosterone-treated myocytes, I_{CaT} was blocked in the biphasic mode, with IC_{50} values of 1.5 and 300 μM (*Figure 1D*), corresponding to the sensitivities described for $Ca_v3.2$- and $Ca_v3.1$-related currents, respectively.[16,17] The relative contributions of these currents were assessed from the Ni^{2+} dose–response relationship, and we found that $Ca_v3.2$ and $Ca_v3.1$ contributed 20 and 80% of the total current, respectively. These relative contributions of functional $Ca_v3.X$ channels correspond to observations reported in pathological conditions.[9]

3.2 Aldosterone increases transcription of the $Ca_v3.1$ gene by activating the GR

Quantitative RT–PCR showed that $Ca_v3.1$ and $Ca_v3.2$ mRNA levels were higher (by factors of 2.4 and 1.4, respectively) in aldosterone-treated cells than in control cells (*Figure 2A*). These results contrast with those of Lalevée *et al.*[13] who found that aldosterone-induced I_{CaT} was associated with an increase in the amount of $Ca_v3.2$ mRNA (up to 410%) and a non-significant increase in the $Ca_v3.1$ mRNA level. This discrepancy is probably due to the use of an inappropriate normalization marker, cyclophilin, which is repressed in aldosterone-treated cells, and the use of primers that do not recognize the relevant isoform (data shown and discussed in Supplementary material online, *Figure S1*). Thereafter, we have focused our study on the regulation of $Ca_v3.1$ gene expression.

The amount of $Ca_v3.1$ mRNA increased in aldosterone-treated cells, reaching a plateau 9 h after the beginning of treatment (*Figure 2B*). Cycloheximide treatment did not prevent aldosterone-induced increases in mRNA levels during the first hour (Supplementary material online, *Figure S2*), suggesting that aldosterone activated pre-existing regulatory factors. However, protein synthesis was required for a sustained effect of aldosterone, since the $Ca_v3.1$ mRNA amount gradually declined after the first hour of aldosterone plus cycloheximide treatment. The effect of the pre-existing transcriptional factor was no longer visible after 9 h of treatment.

We further assessed *cacna1g* regulation by investigating promoter activity through unidirectional deletions and point mutations. Aldosterone treatment induced an increase in promoter activity, which was maximal for sequences up to 1.5 kb long (pGL4400) (*Figure 2C*). Aldosterone had a dose-dependent effect on $Ca_v3.1$ upregulation, and we found that when compared with control, 1 μM induced an 87% increase of pGL4400 activity and 0.1 μM only 20% increase of pGL4400 activity (Supplementary material online, *Figure S3*).

Treatment with the GR antagonist RU 38486 almost completely turned off the transcription of pGL4400 (and pGL4600, data not shown) in both aldosterone-treated and untreated cells (*Figure 2D*). In contrast, the mineralocorticoid receptor (MR) antagonist spironolactone simply decreased the level of transcription. Several putative glucocorticoid response elements (GREs) are present in pGL4400.[14] Mutations in GRE1 abolished aldosterone-induced transcription of the $Ca_v3.1$ gene, *cacna1g* (*Figure 2E*), but did not alter basal levels of transcription or the levels of transcription induced by a synthetic glucocorticoid analogue, dexamethasone. Consistent with these findings, the rapid (10 min) translocation of GR from the cytosol to the nuclear compartment (*Figure 2F*) was observed in aldosterone-treated cells, supporting the role of GR in the genomic response of aldosterone. After 2 h of incubation with aldosterone, the amount in cytosolic GR returned to control levels, probably due to *de novo* GR synthesis. These findings are consistent with the involvement of pre-existing regulatory factors and the need for *de novo* synthesis for sustained increases in mRNA levels.

3.3 I_{CaT} modulates *cacna1g* expression and CREB activation

To test the hypothesis that I_{CaT} is likely to play a role in the control of gene expression, we investigated the effect of the I_{CaT} blockers

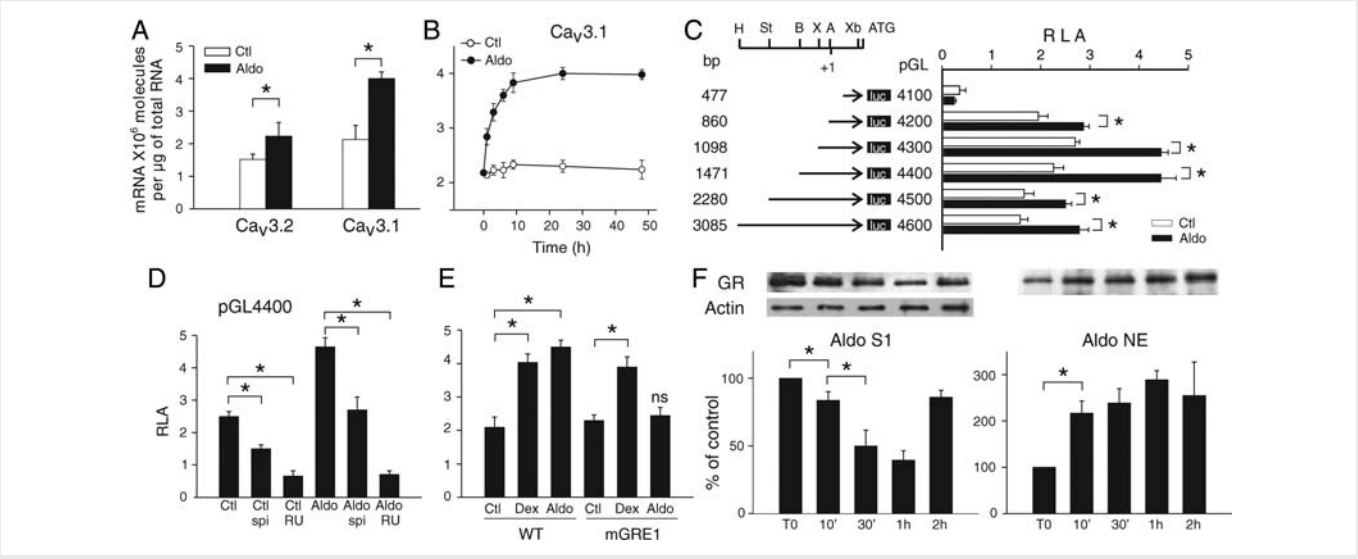

Figure 2 Aldosterone increases $Ca_v3.1$ expression by activating GRs. (*A*) Quantitative RT–PCR of Ca_v3 subunits in cells treated by 1 μM aldosterone for 24 h, $n = 5$ for each point. (*B*) Increase in $Ca_v3.1$ mRNA levels over time, $n = 4$ performed in duplicate for each point. (*C*) *cacna1g* promoter activity. *Age*I (A), *Bgl*II (B), *Hin*dIII (H), *Stu*I (St), *Xba*I (Xb) and *Xho*I (X). Mean relative luciferase activity (RLA) units ± SE. (*D*) Effect of spironolactone (spi, 10 μM) and RU 38486 (RU, 10 μM) on pGL4400-transfected cells. $n = 3$ performed in triplicate. (*E*) Identification of the functional GRE in *cacna1g* promoter. Cells were transfected with either wild-type pGL4400 (WT) or mutated pGL4400-GRE1 (mGRE1) and exposed to 1 μM aldosterone or 10 μM dexamethasone (Dex), $n = 3$ performed in triplicate. (*F*) Nuclear translocation of GRs in aldosterone-treated cells. Western blots were performed with cytosolic (S1, $n = 3$) and nuclear extracts (NE, $n = 3$) performed in triplicate. *$P < 0.05$, ns vs. Ctl.

mibefradil, fluoxetine, and flunarizine[18–20] on *cacna1g* expression (*Figure 3A*). During the exponential phase of mRNA accumulation (until 6 h—*Figure 2B*), Ca^{2+} current blockers had no effect on the amount of $Ca_v3.1$ mRNA (*Figure 3A*). However, during the plateau phase (9 h), $Ca_v3.1$ mRNA levels were higher with aldosterone plus mibefradil (AM) or flunarizine (AFluna) [or fluoxetine (AFluo), data not shown] than with aldosterone alone. Blocking I_{CaL} with nifedipine had no additional effect. The aldosterone-induced increase in I_{CaT} density triggered negative feedback control over *cacna1g* expression that was confirmed by the stronger promoter activity observed in pGL4400-transfected cells exposed to AM than in transfected cells exposed to aldosterone alone (*Figure 3B*). We then focused on the transcription factors regulated by I_{CaT}-generated Ca^{2+} influx. As GR can interact with the CREB,[21] we investigated the effect of I_{CaT} blockade on GR translocation and CREB activation. GR translocation was unchanged in cells exposed to AM or AFluna (Supplementary material online, *Figure S4*). Aldosterone induced a rapid increase in Ser133-phosphorylated CREB protein levels in the nucleus (*Figure 3C*), and aldosterone-induced CREB activation was doubled by I_{CaT} blockade (*Figure 3D*). The level of total CREB remained stable within these culture conditions (data not shown).

Finally, we used a rat model of abdominal aortic stenosis to examine the possible relationship between I_{CaT} and CREB phosphorylation in pathological conditions. We have previously shown that I_{CaT} only re-emerges after long-term stenosis, well after the establishment of compensated hypertrophy. Indeed, I_{CaT} was absent 6 weeks after the induction of stenosis and re-emerged after 12 weeks of stenosis.[9] We show here that CREB phosphorylation levels were increased in the 6-week stenosis group compared with the sham-operated group, whereas CREB phosphorylation was almost abolished in the 12-week stenosis group (*Figure 3E*). Decrease in CREB phosphorylation was prevented in conditions in which I_{CaT} re-expression was diminished (Supplementary material online, *Figure S5*).

3.4 I_{CaT} modulates CREB activation via PP2A

Many signalling pathways are thought to control CREB phosphorylation status, depending on cell and physiopathological status.[22] We investigated the involvement of the serine threonine phosphatases 1, 2A, and 2B (PP1, PP2A, and PP2B), to identify the protein phosphatases modulating CREB activation during aldosterone treatment (*Figure 4*). Cells were treated with the PP2B (calcineurin) inhibitor FK506 (1 μM) or with the PP2A inhibitor OA (5 nM) (*Figure 4A*). OA treatment increased phosphorylated CREB levels in control and aldosterone-treated cells. In contrast, FK506 treatment prevented the aldosterone-induced increase in phosphorylated CREB levels but had no effect on these levels in control cells. Neither OA nor FK506 affected total CREB levels (data not shown).

PP2A and PP1 activities were determined *in vitro* for cardiomyocyte lysates and could be separated on the basis of sensitivity to OA concentration (*Figure 4B*). In aldosterone-treated cells, total PP2A–PP1 activity was twice that in control cells, mostly due to an increase in PP2A activity. Indeed, 80 ± 5% of phosphatase activity was abolished by PP2A blockade (OA—12 nM). The aldosterone-induced increase in PP2A–PP1 activity was prevented by the I_{CaT} blockers. The small contribution of PP1 in aldosterone-treated cells was confirmed using an inhibitor of PP1, and its activation shown to depend on I_{CaT}-generated Ca^{2+} signalling (*Figure 4B*, *bottom panel*). Finally, we were unable to detect a significant difference in the amounts of the catalytic subunits of PP1, PP2A, and PP2B, under the different culture

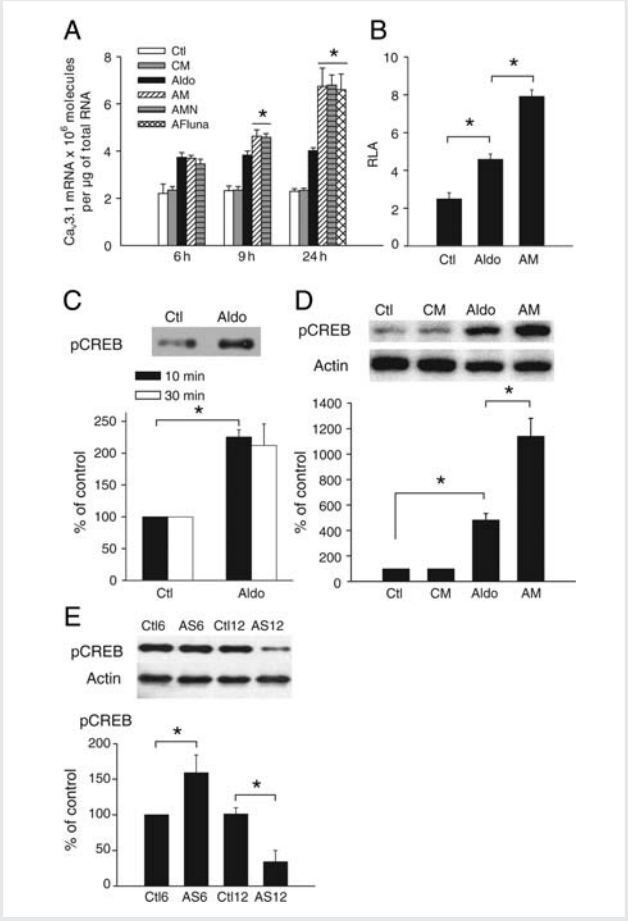

Figure 3 I_{CaT} blockade upregulates *cacna1g* expression and increases pCREB protein levels. (*A*) Effect of I_{CaT} blockade on the increase in $Ca_v3.1$ mRNA levels over time. Cells were cultured with 1 µM mibefradil (CM), mibefradil plus 1 µM aldosterone (AM), mibefradil plus aldosterone and 5 µM nifedipine (AMN) or with aldosterone, and 10 µM flunarizine (AFluna), for the times indicated. $n = 4$ for each condition, $^*P < 0.05$ vs. aldosterone. (*B*) Effect of 1 µM mibefradil on pGL4400 activity, $n = 3$ performed in triplicate. (*C*) Nuclear translocation of phosphorylated CREB. Western blots were performed with nuclear extracts from cells subjected to short-term aldosterone treatment. $n = 4$ performed in duplicate. (*D*) Effect of I_{CaT} blockade on CREB activation. Western blots were performed with total protein extracts from cells treated for 24 h. $n = 3$ performed in duplicate. (*E*) Phosphorylated CREB levels in the pathological model. Western blots were performed with total protein extracts from left ventricles of 6 ($n = 4$) or 12 ($n = 6$) weeks stenosed rats (AS6 and AS12) paired with sham-operated rats (Ctl6, $n = 4$ and Ctl12, $n = 5$). $^*P < 0.05$.

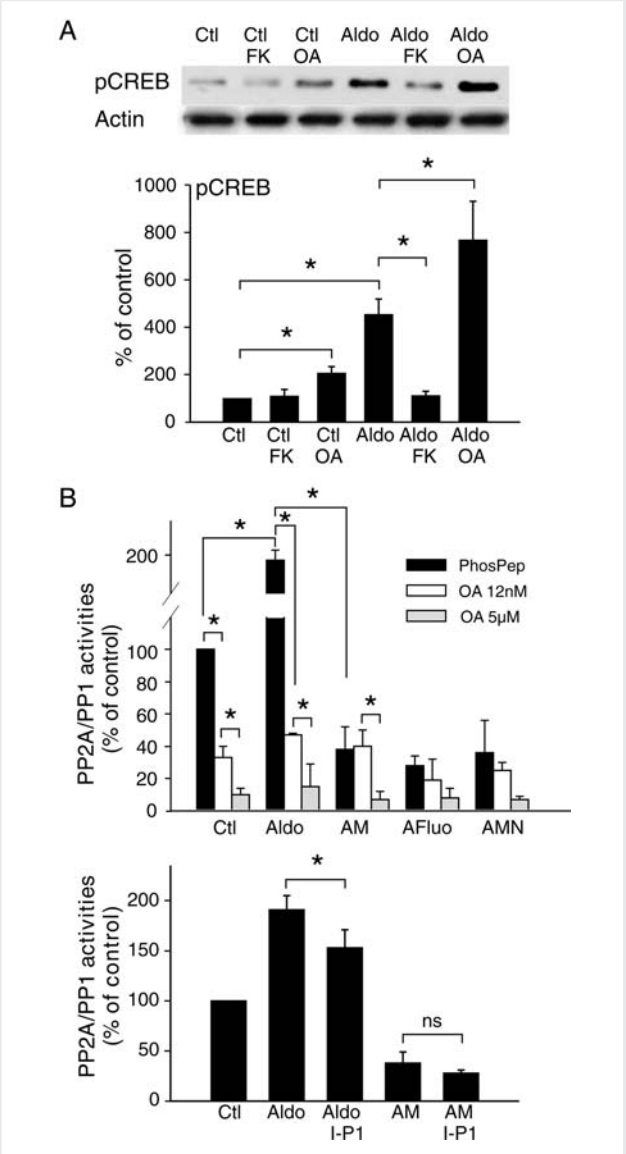

Figure 4 I_{CaT} blockade decreases PP2A-induced CREB dephosphorylation. (*A*) Effect of PP2A and PP2B on CREB phosphorylation. Total proteins were extracted from cells exposed for 24 h to 1 µM FK506 (FK) or 5 nM okadaic acid (OA). $n = 3$ performed in duplicate. (*B*) Aldosterone increases PP2A–PP1 activities via I_{CaT} signalling. Total PP2A and PP1 activities were quantified in cells treated for 24 h with 1 µM aldosterone and 1 µM mibefradil or 5 µM fluoxetine (AM, AFluo) or I_{CaT} and I_{CaL} blockers (AMN); 12 nM OA blocked PP2A activity and 5 µM OA blocked PP2A and PP1 activities. Protein phosphatase inhibitor-2 (I-P1) blocked PP1 activity. PhosPep = 0.1 mM phosphopeptide alone. $n = 3$ performed in triplicate. $^*P < 0.05$.

conditions tested (Supplementary material online, *Figure S6*). Therefore, aldosterone-induced I_{CaT} upregulates the level of phosphatase activity through post-transcriptional regulation rather than changes in phosphatase gene expression.

3.5 I_{CaT} modulates cell-death markers via PP2A

An increase in PP2A activity was associated with cell death.[23] We investigated whether I_{CaT}-induced PP2A activity might be involved in cardiomyocyte death (*Figure 5*). An increase in activated caspase 9 levels occurred only 9 h after the start of the treatment (*Figure 5A*) in parallel with a time-dependent effect of I_{CaT} blockade (*Figure 3A*). At this time point, treatment with OA prevented the aldosterone-induced caspase 9 activation. Aldosterone also induced a switch between the Bcl-x_L and Bcl-x_S variants, which was prevented by the use of OA or OA plus mibefradil (*Figure 5B*). These results indicated that the timing of PP2A activation was related to an increase in I_{CaT}-generated Ca^{2+} influx. The relationship between I_{CaT} and the activation of pro-apoptotic markers was confirmed in cells treated for 24 h with aldosterone, in which the increase in caspase 9 and

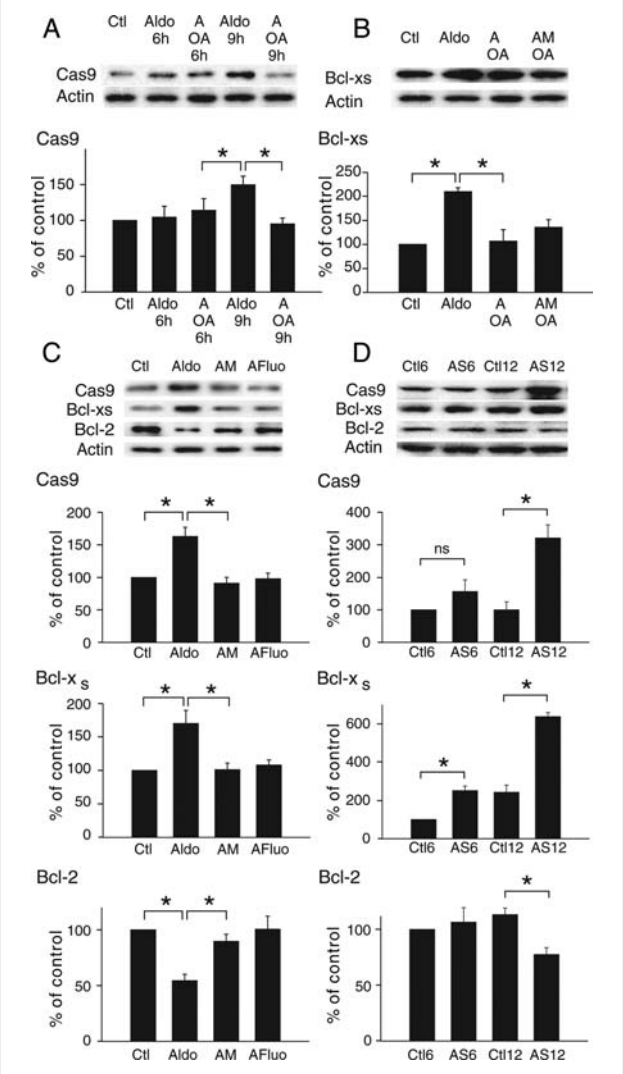

Figure 5 Aldosterone induces pro-apoptotic markers via PP2A. (*A*) Aldosterone-induced time-dependent activation of caspase 9. Cells exposed to 1 μM aldosterone were treated with 5 nM OA (A OA) for the time periods indicated. $n = 3$ performed in duplicate. (*B*) Aldosterone-induced increase in the Bcl-x_S variant via PP2A. Cells were exposed for 9 h to 1 μM aldosterone, together with 5 nM OA (A OA) or 1 μM mibefradil + 5 nM OA (AM OA). $n = 3$ performed in duplicate. (*C*) Effect of I_{CaT} blockers on the aldosterone-induced increase in apoptotic markers in cells treated for 24 h. $n = 3$ performed in duplicate. (*D*) Expression of apoptotic markers in the pathological model. Proteins were extracted from left ventricles of 6- and 12-week stenosed rats paired with control. Ctl6 and AS6 $n = 4$, Ctl12 $n = 5$ and AS12 $n = 6$. $^*P < 0.05$.

Bcl-x_S levels and the decrease in Bcl-2 levels were reversed by treatment with mibefradil or fluoxetine (*Figure 5C*).

Finally, using a rat model of cardiac hypertrophy, we have shown in long-term stenosis (12 weeks treatment—AS12) that the levels of caspase 9 and Bcl-x_S markedly increased, whereas the reciprocal effect was seen on Bcl-2, when compared with the sham group (Ctl12) (*Figure 5D*). Only the levels of Bcl-x_S increased during hypertrophy (6 weeks treatment—AS6 vs. Ctl6) or ageing (Ctl12 vs. Ctl6).

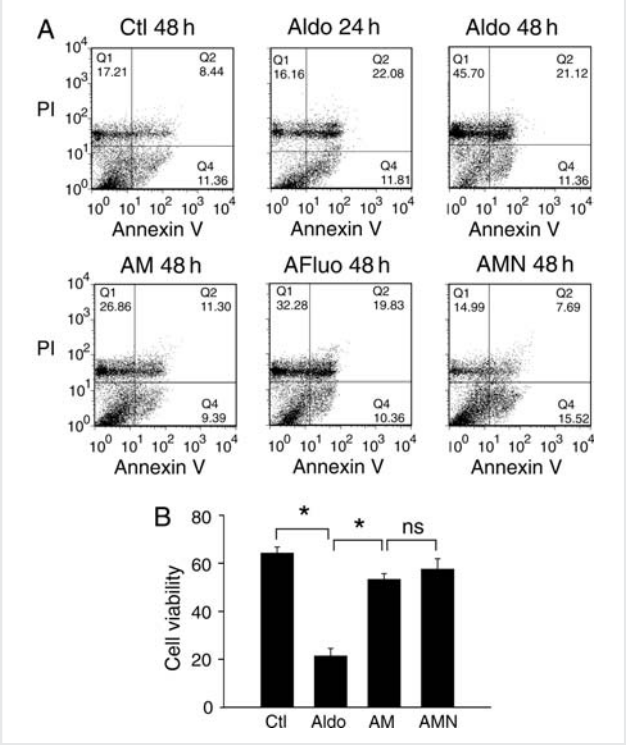

Figure 6 I_{CaT} blockade reduces aldosterone-induced myocyte apoptosis and necrosis. (*A*) Representative graphs from flow cytometry analysis. Cells were treated for the indicated periods before annexin V-FITC/PI double staining. Q1 = annexin V-negative/PI-positive, Q2 = annexin V-positive/PI-positive, Q3 = annexin V-negative/PI-negative and Q4 = annexin V-positive/PI-negative. Annexin V and PI labelled pro-apoptotic and necrotic cells, respectively. (*B*) Cell viability from annexin V-negative/PI-negative stained cells. Clt and Aldo 48 h $n = 6$, Aldo 24 h and AMN $n = 4$, AM and AFluo $n = 5$. $^*P < 0.05$.

3.6 Aldosterone-induced I_{CaT} contributes to myocyte apoptosis and necrosis

Apoptosis was quantified by FACS analysis after staining with annexin V-FITC and PI. As previously reported,[24] aldosterone induced cardiomyocyte apoptosis in cells treated for 24 h, as shown by flow cytometry (annexin V-stained cells, Q2 + Q4) (*Figure 6A*). However, longer periods of exposure to aldosterone (48 h) increased the number of necrotic PI-stained cells (Q1) ($P < 0.05$ vs. Q1 aldosterone 24 h), whereas no significant difference was found in the number of annexin V—or annexin V + PI-stained cells (Q2 + Q4) between 24 and 48 h of aldosterone exposure. Treatment with AM decreased the effect of aldosterone on cell death, as shown by smaller numbers of necrotic cells ($P < 0.05$, Q1 AM vs. Q1 aldosterone 48 h) and apoptotic cells ($P < 0.05$, Q2 + Q4 AM vs. Q2 + Q4 aldosterone 48 h). Treatment with AFluo also reduced the number of necrotic cells ($P < 0.05$, Q1 AFluo vs. Q1 aldosterone 48 h) but did not significantly reduce the number of annexin V-stained cells (Q2 + Q4) vs. (Q2 + Q4) aldosterone 48 h. The use of nifedipine in addition to aldosterone plus mibefradil (AMN) enhanced the effect of AM reducing further the number of PI-stained cells ($P < 0.05$, Q1 AMN vs. Q1 AM and Q1 AMN vs. Q1 aldosterone 48 h). In conclusion, the use of mibefradil with or without nifedipine

reversed the effect of aldosterone on cell viability (*Figure 6B*). Thus, aldosterone-dependent apoptosis and necrosis are induced by both I_{CaT} and I_{CaL}.

4. Discussion

We have investigated the signalling pathway(s) of I_{CaT} and its implication in cardiomyocyte death. In this context, we have focused on the pathway(s) by which aldosterone upregulates $Ca_v3.1$ expression to generate I_{CaT} and identified mechanisms involved in *cacna1g* expression.

We show here that, in neonatal cardiomyocytes, aldosterone-induced increase in I_{CaT} density results mostly from an increase in $Ca_v3.1$ expression. The transactivation of *cacna1g* by GR was observed with either aldosterone or dexamethasone (1 μM), but aldosterone-activated GRs targeted a GRE (GRE1) that is different from those targeted by dexamethasone-activated GRs. The aldosterone-induced increase in I_{CaT}-generated Ca^{2+} signalling led to molecular remodelling. Indeed, we found that aldosterone-induced CREB phosphorylation was altered by I_{CaT}-generated Ca^{2+} signalling, likely resulting in a reduced transcription of CREB's target genes. I_{CaT}-signalling also exerts a negative feedback regulation on *cacna1g* expression, which occurs only after exposure to aldosterone for 9 h, suggesting that functional channels are not present at the membrane before that time. While there is still insufficient evidence to infer the existence of a direct interaction between CREB and the GR-binding *cacna1g* promoter, it seems likely that the I_{CaT}-induced decrease in *cacna1g* expression is due to a defect in CREB interference with the GR-binding activity of GRE1. Further investigations of this issue are required.

We also found that the decrease in phosphorylated CREB levels was mediated by an I_{CaT}-induced increase in PP2A and, to a lesser extent, to PP1 activities. However, PP2B exerts opposite effects on CREB phosphorylation because PP2B blockade prevented aldosterone-induced CREB phosphorylation without affecting the total amount of CREB, therefore excluding the possibilities of an increase in ubiquitination and the degradation of phosphorylated CREB.[22] In the heart, several isoforms of phosphodiesterase (PDE) hydrolyze cAMP and cGMP,[25] and the activities of these enzymes are modulated by phosphorylation.[26] Therefore, PP2B blockade may decrease CREB activation by inhibiting PDE dephosphorylation, thereby increasing PDE activity. Indeed, the inhibition of PDE4 was shown to elicit cAMP/protein kinase A-dependent CREB phosphorylation in cardiac cells.[27] A priori, our results differ from those describing an inhibitory effect of aldosterone-activated MRs on CREB phosphorylation through PP2B in vascular smooth muscle cells.[28] However, in cardiomyocytes, the response to aldosterone is mediated mostly by GRs and our results are thus consistent with the reported positive effect of dexamethasone-activated GRs on CREB signalling.[28]

A cross-talk between I_{CaT} and CREB signalling is consistent with their opposite expression profiles, together with their antagonistic physiological functions. I_{CaT} and CREB signalling do not seem to be critical for normal cardiac function[8,29] but, in pathological conditions, CREB signalling was implicated in angiotensin II-induced hypertrophy.[30] Stenosis-induced hypertrophy showed an opposite pattern in terms of I_{CaT} re-emergence and CREB activation. Indeed, hypertrophied cardiomyocytes in the rat 6-week-stenosis model displayed an increase in phosphorylated CREB levels. The phosphorylation of CREB was almost abolished in the 12-week stenosis group and coincided with I_{CaT} re-emergence. In addition, when the re-emergence of I_{CaT} is reversed, the decrease in I_{CaT} density is correlated with a re-increase in phosphorylated CREB protein levels. Therefore, the negative feedback of I_{CaT} on CREB signalling observed in neonatal cardiomyocytes also seems to occur in pathological conditions in the adult. This result also suggests that I_{CaT} signalling renders cardiomyocytes resistant to hypertrophic factor-induced CREB signalling in the later stages of cardiac hypertrophy. Thus, loss of the negative feedback regulation of CREB signalling by I_{CaT} may partly account for the hypersensitivity to hypertrophy described for $Ca_v3.1^{-/-}$ mice.[8]

The CREB and I_{CaT}-signalling pathways have opposite effects on cell proliferation. For example, I_{CaT} signalling and CREB signalling have antagonistic effect on the pathway mediated by cell-cycle inhibitor p21CIP1.[31] This feature is particularly important in heart, as recent study has reported the persistence in adolescent heart of immature cardiomyocytes with I_{CaT}-generated Ca^{2+} influx.[32] The CREB and I_{CaT}-signalling pathways also have opposite effects on cell-death processes. CREB signalling was presumed to have anti-apoptotic effects through the upregulation of Bcl-2[33] and the prevention of NO-induced apoptosis.[27] Conversely, the activities of PP2A and PP1 have been associated with cell apoptosis.[23] Our study shows that, in aldosterone-treated cardiomyocytes, I_{CaT}-induced PP2A activation increases the expression of pro-apoptotic markers, such as caspase 9 and the Bcl-xS variant. Consistent with these findings, cardiomyocyte apoptosis was first detected 24 h after aldosterone exposure and the longer term (48 h) effects of aldosterone involve an increase in necrosis rather than apoptosis. The blockade of I_{CaT}-generated Ca^{2+} signalling decreases cell death by reducing both apoptosis and necrosis, whereas, as previously reported,[34] the blockade of I_{CaL} decreases necrosis rather than apoptosis. Aldosterone therefore induces different signalling pathways through Ca^{2+} microdomains, related to either I_{CaT}- or I_{CaL}-generated Ca^{2+} influx, such as the activation of PP2A–PP1 or PP2B,[24] respectively, resulting in temporally regulated cell processes. Consistent with this idea, an increase in the levels of apoptotic markers in the pathological model was associated with the re-emergence of I_{CaT} in long-term stenosis (Supplementary material online, *Figure S5*). Nevertheless, further investigation will be needed to confirm the relationship between PP2A and CREB dephosphorylation in adult rat during heart pathology.

In conclusion, the main finding of our study is that the increase in I_{CaT} density induces Ca^{2+} signalling, which targets PP2A–PP1 and results in a downregulation of CREB target genes such as those associated with cardiac hypertrophy. Through its targeting of PP2A–PP1, I_{CaT} increases pro-apoptotic markers and cell death. Although neonatal cardiomyocytes in culture do not completely reflect what takes place in the adult, we confirm that the re-emergence of I_{CaT} in a long-term cardiac hypertrophy model is associated with the reduction of CREB-mediated gene expression and the stimulation of expression of apoptotic markers. Thus, our results suggest that, during cardiac pathology, I_{CaT} may limit the progression of hypertrophy, thereby corroborating the conclusion of Nakayama *et al.*[8] Whether or not cell death induced by I_{CaT} has a 'protective' effect against heart disease, such as described by Nakayama *et al.*, is difficult to reconcile and needs to be further investigated. However, it is noteworthy that the protective effect of I_{CaT} described by Nakayama *et al.* occurs via an NOS3-dependent signalling, the product of which was shown to result in cardiomyocyte apoptosis.[35] The I_{CaT}/PP2A/CREB signalling pathway, described in this study, may represent an

alternative to I_{CaT}/NOS3/PKG1 signalling pathway involved in the anti-hypertrophic effect of I_{CaT} during heart pathology.

5. Limitations

Most papers describing an effect of aldosterone on ionic currents in cardiomyocyte use a concentration of 1 μM aldosterone, and we found that 1 μM Aldo was indeed the most potent concentration for upregulating the promoter of the *cacna1g* gene. We should point out that 1 μM aldosterone is approximately two orders of magnitude higher than physiological concentration. However, *in vivo*, the impact of paracrine effects, such as those of the renin–angiotensin II–aldosterone system, which is thought to occur in the heart,[36] cannot be ignored. Such effects may locally increase aldosterone concentration and increase the impact of plasma aldosterone concentration.

Supplementary material

Supplementary material is available at *Cardiovascular Research* online.

Acknowledgement

We thank A. Coulombe for his support and Prof. A. C. Dolphin for comments on the manuscript. We also wish to thank A. Capderou for its scientific support and N. Kerlero-de-Rosbo for helpful discussion and critical reading of the manuscript.

Conflict of interest: none declared.

Funding

This work was supported by the Centre National de la Recherche Scientifique, the Association Marie Lannelongue and the Association Française contre les Myopathies (D10581/F11898). Funding to pay the Open Access publication charge was provided by Marie Lannelongue hospital.

References

1. Lory P, Bidaud I, Chemin J. T-type calcium channels in differentiation and proliferation. *Cell Calcium* 2006;**40**:135–146.
2. Cribbs LL. T-type Ca2+ channels in vascular smooth muscle: multiple functions. *Cell Calcium* 2006;**40**:221–230.
3. Vassort G, Talavera K, Alvarez JL. Role of T-type Ca2+ channels in the heart. *Cell Calcium* 2006;**40**:205–220.
4. Cribbs LL, Martin BL, Schroder EA, Keller BB, Delisle BP, Satin J. Identification of the T-type calcium channel (Ca(v)3.1d) in developing mouse heart. *Circ Res* 2001;**88**:403–407.
5. Ferron L, Capuano V, Deroubaix E, Coulombe A, Renaud JF. Functional and molecular characterization of a T-type Ca(2+) channel during fetal and postnatal rat heart development. *J Mol Cell Cardiol* 2002;**34**:533–546.
6. Niwa N, Yasui K, Opthof T, Takemura H, Shimizu A, Horiba M *et al*. Cav3.2 subunit underlies the functional T-type Ca2+ channel in murine hearts during the embryonic period. *Am J Physiol Heart Circ Physiol* 2004;**286**:H2257–H2263.
7. Chiang CS, Huang CH, Chieng H, Chang YT, Chang D, Chen JJ *et al*. The CaV3.2 T-Type Ca2+ channel is required for pressure overload-induced cardiac hypertrophy in mice. *Circ Res* 2009;**104**:522–530.
8. Nakayama H, Bodi I, Correll RN, Chen X, Lorenz J, Houser SR *et al*. alpha1G-dependent T-type Ca2+ current antagonizes cardiac hypertrophy through a NOS3-dependent mechanism in mice. *J Clin Invest* 2009;**119**:3787–3796.
9. Ferron L, Capuano V, Ruchon Y, Deroubaix E, Coulombe A, Renaud JF. Angiotensin II signaling pathways mediate expression of cardiac T-type calcium channels. *Circ Res* 2003;**93**:1241–1248.
10. Fareh S, Benardeau A, Thibault B, Nattel S. The T-type Ca(2+) channel blocker mibefradil prevents the development of a substrate for atrial fibrillation by tachycardia-induced atrial remodeling in dogs. *Circulation* 1999;**100**:2191–2197.
11. Kinoshita H, Kuwahara K, Takano M, Arai Y, Kuwabara Y, Yasuno S *et al*. T-type Ca2+ channel blockade prevents sudden death in mice with heart failure. *Circulation* 2009;**120**:743–752.
12. Benitah JP, Vassort G. Aldosterone upregulates Ca(2+) current in adult rat cardiomyocytes. *Circ Res* 1999;**85**:1139–1145.
13. Lalevee N, Rebsamen MC, Barrere-Lemaire S, Perrier E, Nargeot J, Benitah JP *et al*. Aldosterone increases T-type calcium channel expression and *in vitro* beating frequency in neonatal rat cardiomyocytes. *Cardiovasc Res* 2005;**67**:216–224.
14. Benmohamed F, Ferron L, Ruchon Y, Gouadon E, Renaud JF, Capuano V. Regulation of T-type Cav3.1 channels expression by synthetic glucocorticoid dexamethasone in neonatal cardiac myocytes. *Mol Cell Biochem* 2009;**320**:173–183.
15. Capuano V, Ruchon Y, Antoine S, Sant MC, Renaud JF. Ventricular hypertrophy induced by mineralocorticoid treatment or aortic stenosis differentially regulates the expression of cardiac K+ channels in the rat. *Mol Cell Biochem* 2002;**237**:1–10.
16. Lee JH, Cribbs LL, Perez-Reyes E. Cloning of a novel four repeat protein related to voltage-gated sodium and calcium channels. *FEBS Lett* 1999;**445**:231–236.
17. Monteil A, Chemin J, Bourinet E, Mennessier G, Lory P, Nargeot J. Molecular and functional properties of the human alpha(1G) subunit that forms T-type calcium channels. *J Biol Chem* 2000;**275**:6090–6100.
18. Martin RL, Lee JH, Cribbs LL, Perez-Reyes E, Hanck DA. Mibefradil block of cloned T-type calcium channels. *J Pharmacol Exp Ther* 2000;**295**:302–308.
19. Traboulsie A, Chemin J, Kupfer E, Nargeot J, Lory P. T-type calcium channels are inhibited by fluoxetine and its metabolite norfluoxetine. *Mol Pharmacol* 2006;**69**:1963–1968.
20. Gackiere F, Bidaux G, Lory P, Prevarskaya N, Mariot P. A role for voltage gated T-type calcium channels in mediating 'capacitative' calcium entry? *Cell Calcium* 2006;**39**:357–366.
21. Sato A, Sheppard KE, Fullerton MJ, Funder JW. cAmp modulates glucocorticoid-induced protein accumulation and glucocorticoid receptor in cardiomyocytes. *Am J Physiol* 1996;**271**:E827–E833.
22. Johannessen M, Delghandi MP, Moens U. What turns CREB on? *Cell Signal* 2004;**16**:1211–1227.
23. Chiang CW, Harris G, Ellig C, Masters SC, Subramanian R, Shenolikar S *et al*. Protein phosphatase 2A activates the proapoptotic function of BAD in interleukin-3-dependent lymphoid cells by a mechanism requiring 14–3–3 dissociation. *Blood* 2001;**97**:1289–1297.
24. Mano A, Tatsumi T, Shiraishi J, Keira N, Nomura T, Takeda M *et al*. Aldosterone directly induces myocyte apoptosis through calcineurin-dependent pathways. *Circulation* 2004;**110**:317–323.
25. Fischmeister R, Castro LR, Abi-Gerges A, Rochais F, Jurevicius J, Leroy J *et al*. Compartmentation of cyclic nucleotide signaling in the heart: the role of cyclic nucleotide phosphodiesterases. *Circ Res* 2006;**99**:816–828.
26. Omori K, Kotera J. Overview of PDEs and their regulation. *Circ Res* 2007;**100**:309–327.
27. Kwak HJ, Park KM, Choi HE, Chung KS, Lim HJ, Park HY. PDE4 inhibitor, roflumilast protects cardiomyocytes against NO-induced apoptosis via activation of PKA and Epac dual pathways. *Cell Signal* 2008;**20**:803–814.
28. Grossmann C, Wuttke M, Ruhs S, Seiferth A, Mildenberger S, Rabe S *et al*. Mineralocorticoid receptor inhibits CREB signaling by calcineurin activation. *FASEB J* 2010;**24**:2010–2019.
29. Matus M, Lewin G, Stumpel F, Buchwalow IB, Schneider MD, Schutz G *et al*. Cardiomyocyte-specific inactivation of transcription factor CREB in mice. *Faseb J* 2007;**21**:1884–1892.
30. Funakoshi Y, Ichiki T, Takeda K, Tokuno T, Iino N, Takeshita A. Critical role of cAMP-response element-binding protein for angiotensin II-induced hypertrophy of vascular smooth muscle cells. *J Biol Chem* 2002;**277**:18710–18717.
31. Lipskaia L, Lompre AM. Alteration in temporal kinetics of Ca2+ signaling and control of growth and proliferation. *Biol Cell* 2004;**96**:55–68.
32. Chen X, Wilson RM, Kubo H, Berretta RM, Harris DM, Zhang X *et al*. Adolescent feline heart contains a population of small, proliferative ventricular myocytes with immature physiological properties. *Circ Res* 2007;**100**:536–544.
33. Maldonado C, Cea P, Adasme T, Collao A, Diaz-Araya G, Chiong M *et al*. IGF-1 protects cardiac myocytes from hyperosmotic stress-induced apoptosis via CREB. *Biochem Biophys Res Commun* 2005;**336**:1112–1118.
34. Nakayama H, Chen X, Baines CP, Klevitsky R, Zhang X, Zhang H *et al*. Ca2+- and mitochondrial-dependent cardiomyocyte necrosis as a primary mediator of heart failure. *J Clin Invest* 2007;**117**:2431–2444.
35. Liao X, Liu JM, Du L, Tang A, Shang Y, Wang SQ *et al*. Nitric oxide signaling in stretch-induced apoptosis of neonatal rat cardiomyocytes. *FASEB J* 2006;**20**:1883–1885.
36. Silvestre JS, Heymes C, Oubenaissa A, Robert V, Aupetit-Faisant B, Carayon A *et al*. Activation of cardiac aldosterone production in rat myocardial infarction: effect of angiotensin II receptor blockade and role in cardiac fibrosis. *Circulation* 1999;**99**:2694–2701.